Characterization of primary cilia features reveal cell-type specific variability in in vitro models of osteogenic and chondrogenic differentiation

Priyanka Upadhyai*, Vishal Singh Guleria* and Prajna Udupa

Department of Medical Genetics, Kasturba Medical College, Manipal, Manipal Academy of Higher Education, Manipal, Karnataka, India

* These authors contributed equally to this work.

ABSTRACT

Primary cilia are non-motile sensory antennae present on most vertebrate cell surfaces. They serve to transduce and integrate diverse external stimuli into functional cellular responses vital for development, differentiation and homeostasis. Ciliary characteristics, such as length, structure and frequency are often tailored to distinct differentiated cell states. Primary cilia are present on a variety of skeletal cell-types and facilitate the assimilation of sensory cues to direct skeletal development and repair. However, there is limited knowledge of ciliary variation in response to the activation of distinct differentiation cascades in different skeletal cell-types. C3H10T1/2, MC3T3-E1 and ATDC5 cells are mesenchymal stem cells, preosteoblast and prechondrocyte cell-lines, respectively. They are commonly employed in numerous in vitro studies, investigating the molecular mechanisms underlying osteoblast and chondrocyte differentiation, skeletal disease and repair. Here we sought to evaluate the primary cilia length and frequencies during osteogenic differentiation in C3H10T1/2 and MC3T3-E1 and chondrogenic differentiation in ATDC5 cells, over a period of 21 days. Our data inform on the presence of stable cilia to orchestrate signaling and dynamic alterations in their features during extended periods of differentiation. Taken together with existing literature these findings reflect the occurrence of not only lineage but cell-type specific variation in ciliary attributes during differentiation. These results extend our current knowledge, shining light on the variabilities in primary cilia features correlated with distinct differentiated cell phenotypes. It may have broader implications in studies using these cell-lines to explore cilia dependent cellular processes and treatment modalities for skeletal disorders centered on cilia modulation.

Subjects Cell Biology, Genetics

Keywords Primary cilia, Osteogenic differentiation, Chondrogenic differentiation, C3H10T1/2, MC3T3-E1, ATDC5, Cilia length and frequency alteration

Submitted 12 March 2020
Accepted 3 August 2020
Published 21 August 2020

Corresponding author
Priyanka Upadhyai,
priyanka.u@manipal.edu

Academic editor
Ursula Stochaj

Additional Information and Declarations can be found on page 16

DOI **10.7717/peerj.9799**

INTRODUCTION

Primary cilia are non-motile sensory organelles that protrude from most mammalian cell surfaces (*Singla & Reiter, 2006*). They transduce various extracellular cues essential for proliferation, differentiation and homeostasis via Hedgehog (Hh), Wnt, Notch, Receptor

Tyrosine Kinase, Transforming growth factor β (TGFβ), G protein-coupled receptor and calcium signaling pathways (*Christensen et al., 2012*; *Clement et al., 2013*; *Ezratty et al., 2011*; *Huangfu et al., 2003*; *Lancaster, Schroth & Gleeson, 2011*; *Nauli et al., 2003*; *Wheway et al., 2015*). The importance of cilia in regulating embryonic and postnatal development is underscored by a wide spectrum of human disorders termed as ciliopathies caused by aberrations in cilia formation and function.

The ciliary backbone or axoneme is a microtubular structure that emanates from a modified centriole, the basal body within the ciliary pocket and is encased in a ciliary membrane contiguous with the plasma membrane of the cell. The transport of proteins into the cilia and the bidirectional intra-ciliary movement of cargo is driven by the intraflagellar transport (IFT) machinery composed of multimeric protein complexes, including but not limited to IFT-A/B complexes and associated motor-proteins, kinesin-2 and dynein 2 (*Berbari et al., 2008*; *Cole et al., 1998*; *Follit et al., 2006*; *Nonaka et al., 1998*; *Omori et al., 2008*; *Pazour, Wilkerson & Witman, 1998*; *Piperno & Mead, 1997*; *Porter et al., 1999*; *Signor et al., 1999*; *Snow et al., 2004*; *Yoshimura et al., 2007*). This not only facilitates the receipt and transduction of signals at the primary cilium but is required for its assembly and maintenance (*Bhogaraju et al., 2013*; *Cole et al., 1998*; *Wren et al., 2013*).

A growing body of evidence has revealed that bone and cartilage are dynamic entities that assimilate a broad range of sensory cues to facilitate skeletal formation and repair. This is augmented by primary cilia extending from the cell surface of osteoblasts, osteocytes, chondrocytes and their precursor preosteoblast and mesenchymal stem cells (MSCs) (*Federman & Nichols, 1974*; *Scherft & Daems, 1967*; *Tummala, Arnsdorf & Jacobs, 2010*). Cilia serve as critical mechanosensors of fluid flow in osteoblasts and osteocytes (*Temiyasathit et al., 2012*), whereas in chondrocytes their main function is sensing peripheral tissue deformation (*McGlashan, Jensen & Poole, 2006*). In this context mechanical stimulation serves as a crucial anabolic signal; it promotes osteogenic (OS) differentiation in MSCs and mineralization of the chondrocyte matrix (*Chen et al., 2015*; *Hoey, Kelly & Jacobs, 2011*; *O'Conor et al., 2014*). Primary cilia are also required for osteoblast, osteocyte polarity, alignment in bone development and regulate chondrocyte cell polarity at the growth plate (*Lim et al., 2020a*; *Song et al., 2007*). They are chemosensitive and serve as a nexus of signaling activity important for OS and chondrogenic (CH) differentiation, such as Hh, TGFβ, Fibroblast growth factor (FGF), Wnt, platelet derived growth factor and parathyroid hormone related peptide (*Cai et al., 2012*; *Caplan & Correa, 2011*; *Chen, Deng & Li, 2012*; *Jiang et al., 2016*; *Kozhemyakina, Lassar & Zelzer, 2015*). The essential role of ciliary function in osteoblast and chondrocyte differentiation is substantiated by impaired differentiation following cilia abrogation caused by knockdown of constituents of the IFT machinery, for example, Ift80, Ift88 and Kif3a (*Qiu et al., 2012*; *Tummala, Arnsdorf & Jacobs, 2010*; *Wang, Yuan & Yang, 2013*; *Yang & Wang, 2012*). Moreover, many ciliopathies manifest with altered cilia length and preponderance, underscoring the importance of cilia in cellular function (*Failler et al., 2014*; *Zhang et al., 2016*).

The basal levels of ciliation and cilia length have been described for several skeletal cell-lines, for example, MC3T3-E1, MLO-Y4, chondrocytes and mesenchymal stem cells

(*Brown et al., 2014*; *Malone et al., 2007*; *Wann & Knight, 2012*; *Xiao et al., 2006*). Ciliary attributes may be tailored in accordance with distinct differentiated cell states. This is corroborated by a previous study that demonstrated lineage specific changes in primary cilia length and frequencies in response to chemically induced differentiation in human MSCs (hMSCs) over a 7 day period (*Dalbay et al., 2015*). Primary cilia length are malleable and modulated by several factors such as cytoskeletal actin organization and inflammatory cytokines (*Kim et al., 2010*; *McMurray et al., 2013*; *Pitaval et al., 2010*; *Wann & Knight, 2012*). Modulation of the anterograde IFT transport speed by intracellular cyclic AMP levels have also been shown to control ciliary length (*Besschetnova et al., 2010*). In chondrocytes compressive loading was reported to reversibly reduce cilia length and incidence (*McGlashan et al., 2010*). Moreover, variable stimulation with growth factors may produce disparate consequences on cilia length. While the constitutive activation of FGF signaling was shown to cause primary cilia shortening, its transient stimulation resulted in cilia elongation, in growth plate chondrocytes and limb bud derived mesenchymal cells (*Kunova Bosakova et al., 2018*; *Martin et al., 2018*).

C3H10T1/2, MC3T3-E1 and ATDC5 are murine mesenchymal stem cells, preosteoblast and prechondrocyte cell-lines, respectively, that are commonly employed in various in vitro studies, interrogating the mechanisms underlying osteoblast and chondrocyte differentiation, bone disorders and repair (*Hino et al., 2018*; *Lee et al., 2017*; *Wang et al., 2019*; *Yao & Wang, 2013*). Despite the wide use of these cell-lines, how ciliary features vary in them during native OS and CH differentiation has not been so far investigated. Here we evaluate the primary cilia length and frequency during OS differentiation in C3H10T1/2 and MC3T3-E1 and CH differentiation in ATDC5 cells, over a period of 21 days. Our study revealed cell-type and lineage specific modulation of ciliary characteristics during extended periods of differentiation. These findings expand our existing knowledge and shine light on the primary cilia features in these cell-lines correlated with distinct differentiated cell fates, and may be significant for clinically relevant and explorative studies evaluating cilia dependent molecular mechanisms in these cellular models.

MATERIALS AND METHODS

Cell culture

ATDC5 cell-line (gift from Dr. Uwe Kornak, Charité—Universitätsmedizin Berlin) were propagated in complete media consisting of DMEM/F-12 (1:1) with 1% L-Glutamine, 10% heat inactivated fetal bovine serum (FBS), one mM sodium pyruvate, 100 U/ml penicillin and 100 µg/ml streptomycin (HiMedia, Mumbai, India). Cells were induced with CH media comprising of complete media supplemented with 10^{-7} M dexamethasone, 50 µg/ml ascorbic acid, 10 mM β glycerophosphate and 1X insulin-transferrin-sodium selenite supplement (all from Sigma–Aldrich, St. Louis, MO, USA). Current method of CH differentiation was adapted from previous studies (*Newton et al., 2012*; *Weiss et al., 2012*). C3H10T1/2 was obtained from the cell repository at National Center for Cell Science, India and MC3T3-E1, sub-clone 4 was a gift from Dr. Uwe Kornak, Charité—Universitätsmedizin Berlin and were cultured in complete media comprising of DMEM and modified Eagle's minimum essential medium, respectively, with 1% L-Glutamine,

10% heat inactivated FBS, one mM sodium pyruvate, 100 U/ml penicillin and 100 µg/ml streptomycin (HiMedia, Mumbai, India). OS media comprised of complete media supplemented with 10^{-7} M dexamethasone, 50 µg/ml ascorbic acid and 10 mM β glycerophosphate. All cells were incubated in a humidified atmosphere (37 °C, 5% CO_2) and media was replaced every second or third day for 21–30 days, as indicated.

Alizarin red staining

Calcium deposition in the extracellular matrix (ECM) was estimated by Alizarin red dye that combines with calcium in the cellular matrix, as described previously (*Ovchinnikov, 2009*; *Yamakawa et al., 2003*). Briefly, cells were seeded in triplicates at the following densities: 18,000/cm^2 (C3H10T1/2), 11,000/cm^2 (MC3T3-E1) and 12,000/cm^2 (ATDC5), respectively in multi-well plates, and were induced ~24 h later with OS or CH differentiation media. Uninduced cells were propagated in complete media for the same period of time as those induced. At 7, 14 and 21 days post differentiation, cells were fixed in 4% paraformaldehyde (PFA) and stained with 2% Alizarin red, pH 4.2 (Sigma–Aldrich, St. Louis, MO, USA) for 40 min at room temperature (RT). Stained monolayers were washed with distilled water and images were captured with inverted phase contrast microscope (Olympus, Tokyo, Japan). Levels of mineralization were quantified by extraction of the stain using 10% (v/v) acetic acid and absorbance was measured at 405 nm (*Gregory et al., 2004*).

Alkaline phosphatase staining

C3H10T1/2 and MC3T3-E1 cells were seeded in triplicates at 18,000/cm^2 and 11,000/cm^2 per well, respectively in multi-well plates. They were induced ~24 h later with OS differentiation media or left uninduced for the same duration as those induced. At 7, 14 and 21 days post differentiation, cells were fixed in 4% PFA, and alkaline phosphatase (*Alp*) was detected by incubating with nitro blue tetrazolium (NBT)/5-bromo-4-chloro-3-indolyl phosphate substrate (Sigma–Aldrich, St. Louis, MO, USA) for up to 30 min at RT. After washing the stained cells with 1X PBS, images were captured using inverted phase contrast microscope (Olympus, Tokyo, Japan).

Alcian blue staining

Glycosaminoglycan (GAG) deposition in the ECM was ascertained following CH differentiation in ATDC5 cells plated at a density of 12,000/cm^2. Subsequently, the cells were fixed in 95% methanol, followed by incubation in 0.1 M HCl and stained with 1% Alcian blue 8GX solution in 3% acetic acid (Sigma–Aldrich, St. Louis, MO, USA). Stained cells were washed with distilled water and images were captured with inverted phase contrast microscope (Axiovert A1 FL; Zeiss, Oberkochen, Germany). Staining intensity was estimated using Fiji (http://imagej.net/Fiji) and represented in arbitrary units.

Primary cilia detection during osteogenic and chondrogenic differentiation

For detection of cilia by immunostaining, cells were seeded on glass coverslips in multi-well plates at the following densities: 18,000/cm^2 (C3H10T1/2), 11,000/cm^2

(MC3T3-E1) and 12,000/cm^2 (ATDC5). They were induced ~24 h later with OS (C3H10T1/2 and MC3T3-E1) or CH (ATDC5) differentiation media and propagated for 7, 14 and 21 days. The uninduced cells were propagated in complete media for the same period of time. To enhance ciliogenesis, all cells were serum starved (ss) as described earlier (*Prosser & Morrison, 2015*). To this end induced and uninduced cells were cultured in differentiation or complete media containing 0.5% FBS for 48 h prior to staining. Two sets of cells were fixed prior to differentiation: one was starved (day 0 uninduced), while the other remained non-starved (day 0 uninduced no ss).

Immunocytochemistry and image analyses

The cells were fixed in 4% PFA, permeabilized in 0.2% Triton X-100, blocked in 5% normal goat serum and finally incubated overnight at 4 °C with primary antibodies—anti-acetylated α tubulin (mouse monoclonal, 1:4,000, cat# T7451; Sigma–Aldrich, St. Louis, MO, USA) and anti-Arl13B (rabbit polyclonal, 1:2,000, cat# 17711-1-AP; ProteinTech, Rosemont, IL, USA) diluted in blocking solution. Cells were incubated in the following secondary antibodies: Alexa fluor 488 goat anti-rabbit and Alexa fluor 568 goat anti-mouse IgG (cat.# A11034 and cat.# A11031; Molecular Probes, Eugene, OR, USA/ThermoFisher Scientific, Waltham, MA, USA), diluted at 1:500 for 2 h at RT. Nuclei were stained using DAPI and mounted in Prolong Diamond Antifade mountant (both from Invitrogen, Carlsbad, CA, USA; ThermoFisher Scientific, Waltham, MA, USA). Images were acquired using an inverted fluorescence microscope equipped with LD Plan-Neofluar 63X/0.75 Corr Ph2 oil immersion objective and Axiocam 503 CCD camera (Axiovert A1 FL; Zeiss, Oberkochen, Germany). Primary cilia were discerned by acetylated α tubulin or Arl13B staining and their length were determined manually by tracing along them using Fiji (http://imagej.net/Fiji). Cilia lengths are represented in micrometer (µm). Immunolabeled entities with a minimal length of 1.5 µm were ascertained as primary cilia. Overall length was assessed for a total of 100–178 cilia in three independent replicates. Ciliary frequencies were evaluated in ~100–200 cells per condition in each of three independent replicates.

Quantitative real time PCR analyses

Cells were seeded at the following densities for RNA extraction: 21,000/cm^2 (C3H10T1/2), 15,000/cm^2 (MC3T3-E1) and 17,000/cm^2 (ATDC5). They were induced ~24 h later with OS (C3H10T1/2 and MC3T3-E1) or CH (ATDC5) differentiation media and propagated for 7, 14 and 21 days. The uninduced cells they were propagated in complete media for the same period of time. All cells were starved as described above. Total RNA was extracted using Trizol reagent (Invitrogen, Carlsbad, CA, USA; ThermoFisher Scientific, Waltham, MA, USA). For each sample, total RNA content was assessed by absorbance at 260 nm and purity by A260/280 ratios, and then reverse transcribed using Superscript IV Vilo mastermix™ (Invitrogen, Carlsbad, CA, USA; ThermoFisher Scientific, Waltham, MA, USA) according to the manufacturer's protocol. Real time quantitative PCR was carried out using StepOne (Applied Biosystems, Foster City, CA, USA; ThermoFisher Scientific, Waltham, MA, USA) with a final reaction volume of 10 µl. All reactions were prepared with five µl of 2x PowerUP™ SYBR™ Green

Table 1 Primers used in qRT-PCR (F: forward; R: reverse).

Gene	Primer sequence (5′–3′)	Tm (°C)	Product size (bp)
Alp	F: CCAACTCTTTTGTGCCAGAGA	58	110
	R: GGCTACATTGGTGTTGAGCTTTT	60	
Runx2	F: CTTTACCTACACCCCGCCAG	60	116
	R: GTCCACTCTGGCTTTGGGAA	60	
Ptch1	F: CCAGCGGCTACCTACTGATG	60	150
	R: TGCCAATCAAGGAGCAGAGG	60	
Sox9	F: TGAAGAACGGACAAGCGGAG	60	198
	R: CAGCTTGCACGTCGGTTTTG	60	
Mmp13	F: GGAGCCCTGATGTTTCCCAT	60	165
	R: ATCAAGGGATAGGGCTGGGT	60	
Gapdh	F: CATGGCCTTCCGTGTTCCTA	60	172
	R: GTTGAAGTCGCAGGAGACAAC	60	

Mastermix (Applied Biosystems, Foster City, CA, USA; ThermoFisher Scientific, Waltham, MA, USA), and run in duplicates for each of three independent replicates. The mRNA levels for target genes were normalized to *GAPDH* using primer sequences indicated in Table 1. Quantification was carried out using the ΔΔCt method.

SAG mediated modulation of Hedgehog signaling

For stimulation with Smoothened (Smo) Agonist (SAG), cells were seeded as described above and propagated in either complete or OS media supplemented with SAG at a final concentration of one μm. Culture media was replaced every second or third day during the period of induction. Cells were ss for 48 h as mentioned above prior to harvesting.

Statistical analyses

Data analyses was performed using GraphPad Prism (v8.4) (www.graphpad.com/scientific-software/prism/). One-way analysis of variance (ANOVA) was performed for identifying variation in cilia length among induced and uninduced groups. Two-way ANOVA was performed to assess effects of day to day variation on induction. Nested *t*-test was performed to evaluate whether induction has an overall effect on cilia length, considering day-wise variation is nested within the induction effect. Primary cilia length, frequencies and gene expression studies were performed in three independent replicates and $p < 0.05$ was considered statistically significant. Cilia length and frequency values are shown as mean ± SEM.

RESULTS

C3H10T1/2, MC3T3-E1 and ATDC5 undergo the anticipated osteogenic and chondrogenic differentiation in vitro

The deposition of minerals in the form of hydroxyapatite in the ECM is a physiological characteristic of hard tissues such as bone and growth-plate cartilage. *Alp* expressed by

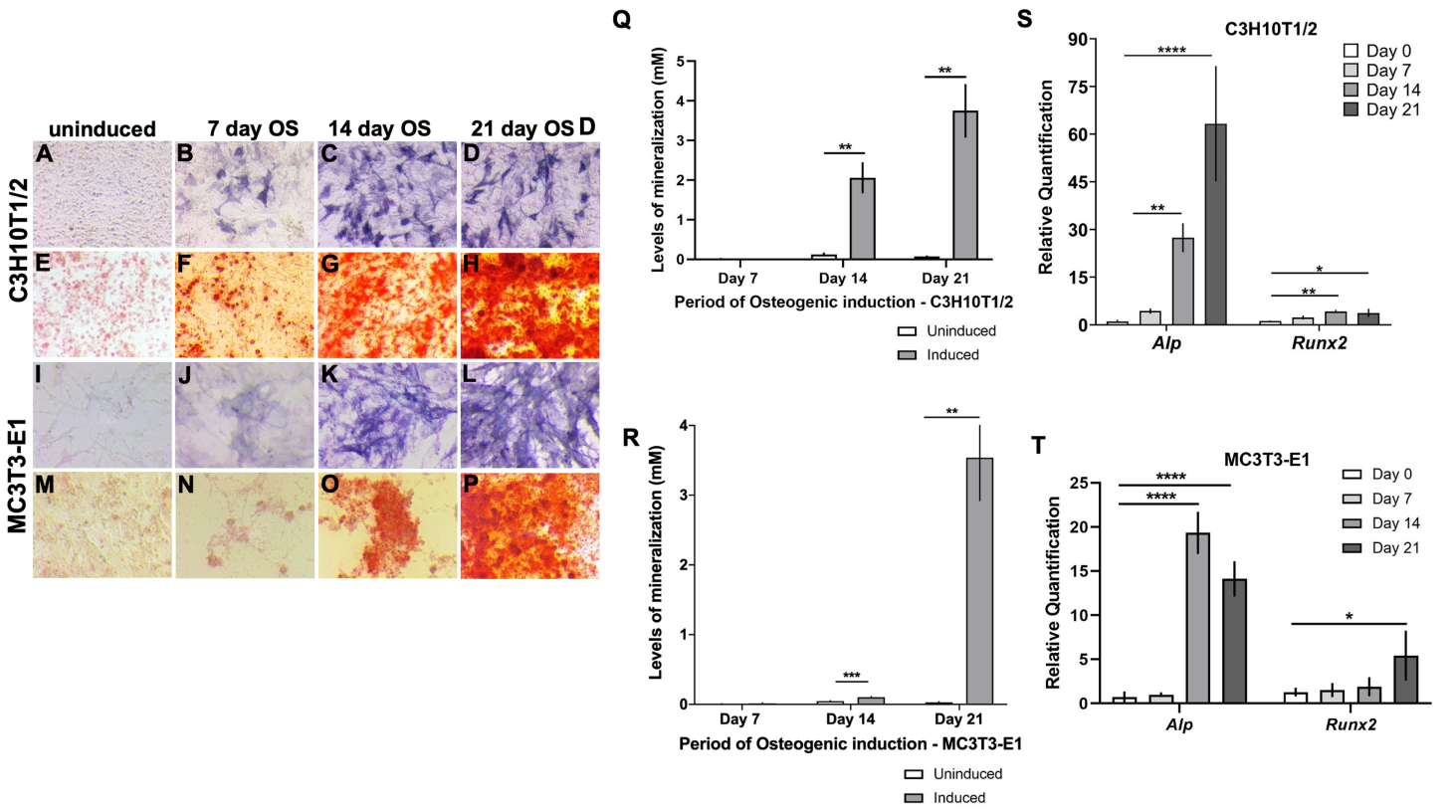

Figure 1 Characterization of in vitro osteogenic differentiation in C3H10T1/2 and MC3T3-E1 cells. (A–P) Enhanced alkaline phosphatase (*Alp*) levels were qualitatively evident in (A–D) C3H10T1/2 and (I–L) MC3T3-E1 cells at 14 and 21 days post osteogenic (OS) induction compared to uninduced. Similarly robust calcium deposition in the ECM was revealed by Alizarin red staining (ARS) in (E–H) C3H10T1/2 and (M–P) MC3T3-E1 cells at 14 and 21 days following OS induction. (Q and R) Quantitative mineralization levels based on ARS confirmed significantly higher extracellular calcium deposition at 14 and 21 days following OS induction compared to day matched uninduced cells in (Q) C3H10T1/2 and (R) MC3T3-E1 cells ($^{**}p < 0.01$, $^{***}p < 0.001$; Two-way ANOVA followed by Sidak's post hoc test). (S and T) qRT-PCR analyses of the transcript levels of OS differentiation markers, *Alp* and *Runx2*. Levels were normalized to *Gapdh* ($^{*}p < 0.05$, $^{**}p < 0.01$, $^{****}p < 0.0001$; One-way ANOVA followed by Tukey's post hoc analyses). (S) In C3H10T1/2, *Alp* and *Runx2* are significantly upregulated at 14 and 21 day OS differentiated cells (T) In MC3T3-E1, *Alp* levels were elevated after 14 and 21 days of OS induction, however, significantly appreciable *Runx2* was detected 21 days following induction.
Full-size DOI: 10.7717/peerj.9799/fig-1

osteoblasts and hypertrophic chondrocytes hydrolyzes pyrophosphate to generate inorganic phosphate to promote matrix mineralization (*Orimo, 2010*). Consequently, high levels of Alp and matrix mineralization reflect osteogenic differentiation. C3H10T1/2 and MC3T3-E1 cells showed elevated OS differentiation following induction from day 14 onward, evidenced qualitatively by pronounced Alp staining in C3H10T1/2 (Figs. 1A–1D) and MC3T3-E1 (Figs. 1I–1L). Elevated calcium deposits in OS induced vs uninduced cells were revealed using Alizarin red staining (ARS) in C3H10T1/2 (Figs. 1E–1H) and MC3T3-E1 (Figs. 1M–1P). Quantitative estimation revealed significant increase in matrix mineralization by day 14 post OS induction that was further enhanced in 21 day induced monolayers (Figs. 1Q and 1R). We evaluated the transcript levels of osteoblast differentiation markers, *Alp* and *Runx2* by qRT-PCR and found that both were significantly upregulated at 14 and 21 days post OS induction in C3H10T1/2 (Fig. 1S).

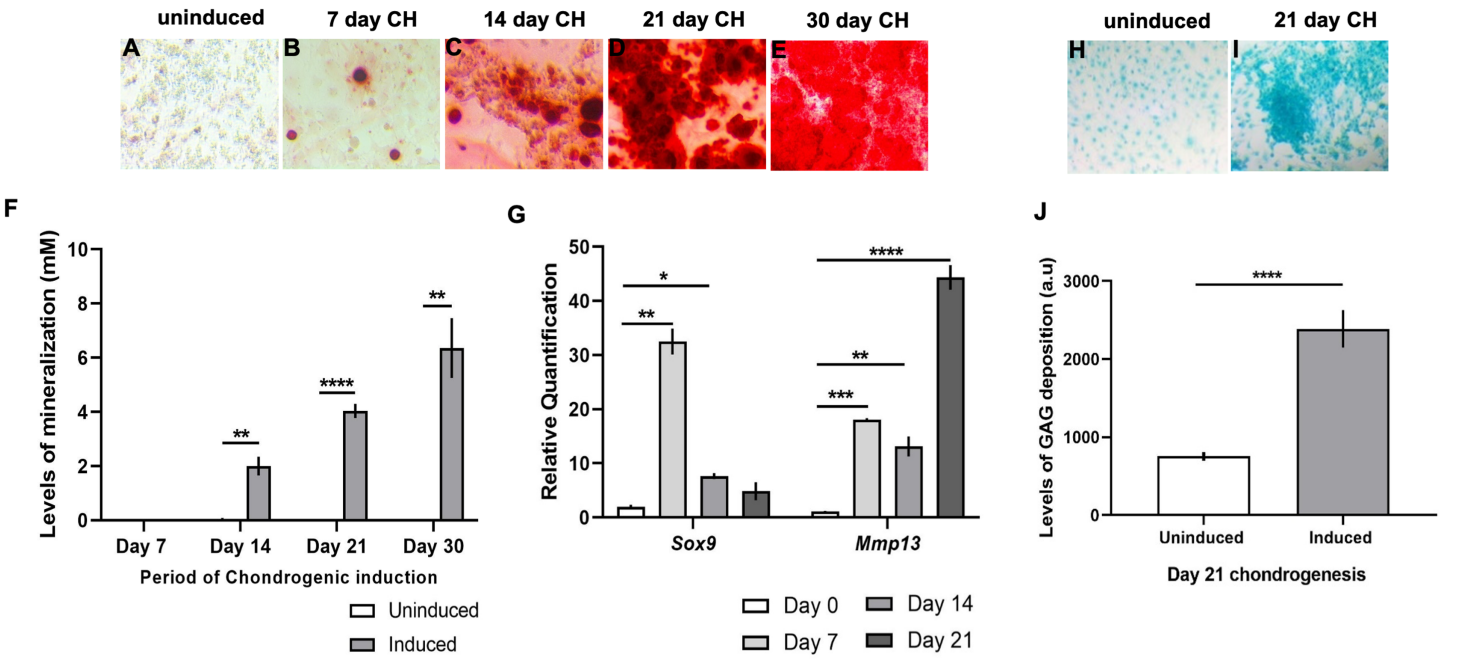

Figure 2 Characterization of chondrogenic differentiation in ATDC5 cells. (A–F) ARS mediated detection of calcium deposition in the ECM following chondrogenic (CH) induction of ATDC5 cells revealed (A–E) perceptible mineralization day 7 onward. (F) Quantitative assessment confirmed significantly high mineralization levels in CH induced monolayers at 14, 21 and 30 days as compared to uninduced cells ($^{**}p < 0.01$, $^{****}p < 0.0001$; Two-way ANOVA followed by Sidak's post hoc test). (G) qRT-PCR analyses revealed significant upregulation of the transcript levels of CH marker *Sox9* at 7 and 14 days following differentiation ($^{*}p < 0.05$, $^{**}p < 0.01$; One-way ANOVA followed Dunnett's post hoc test), while CH hypertrophy marker *Mmp13* was elevated at 7, 14 and 21 days following differentiation ($^{**}p < 0.01$, $^{***}p < 0.001$, $^{****}p < 0.0001$; One-way ANOVA followed by Tukey's post hoc analyses). Transcript levels were normalized to *Gapdh*. (H–J) Significantly high extracellular glycosaminoglycan (GAG) deposition was detected at 21 days post CH induction ($^{****}p < 0.0001$; Wilcoxon signed rank test). Full-size DOI: 10.7717/peerj.9799/fig-2

In MC3T3-E1, significantly high *Alp* levels were detected at 14 and 21 days post induction, while elevated *Runx2* was detected at day 21 after OS stimulation (Fig. 1T).

ATDC5 cells, when induced for CH differentiation, showed progressive increase in mineral deposition in the ECM from day 14 onward (Figs. 2A–2E), evidenced by quantification of ARS in the induced cellular monolayers as compared to uninduced (Fig. 2F). Transcript levels of *Sox9*, an early marker of CH differentiation was significantly elevated at 7 and 14 days post CH induction and was subsequently diminished at day 21 (Fig. 2G). *Mmp13*, a marker of chondrocyte hypertrophy was upregulated after 7 days of CH media stimulation but was most strongly induced in 21 day CH induced monolayers (Fig. 2G). CH differentiated cells also showed significant GAG deposition in the ECM at 21 days after treatment, revealed by Alcian blue staining (Figs. 2H–2J). Given that cells were seeded at a moderately higher density for gene expression analyses as compared to other assays, we compared cell proliferation using Trypan blue in C3H10T1/2. Cells were seeded at a density of 21,000/cm^2 on plastic vs 18,000/cm^2 on glass coverslips, followed by OS induction for 2, 4, 6, 8, 10, 12 days. No significant variability was observed in viable cell numbers between the two substrates (Fig. S1).

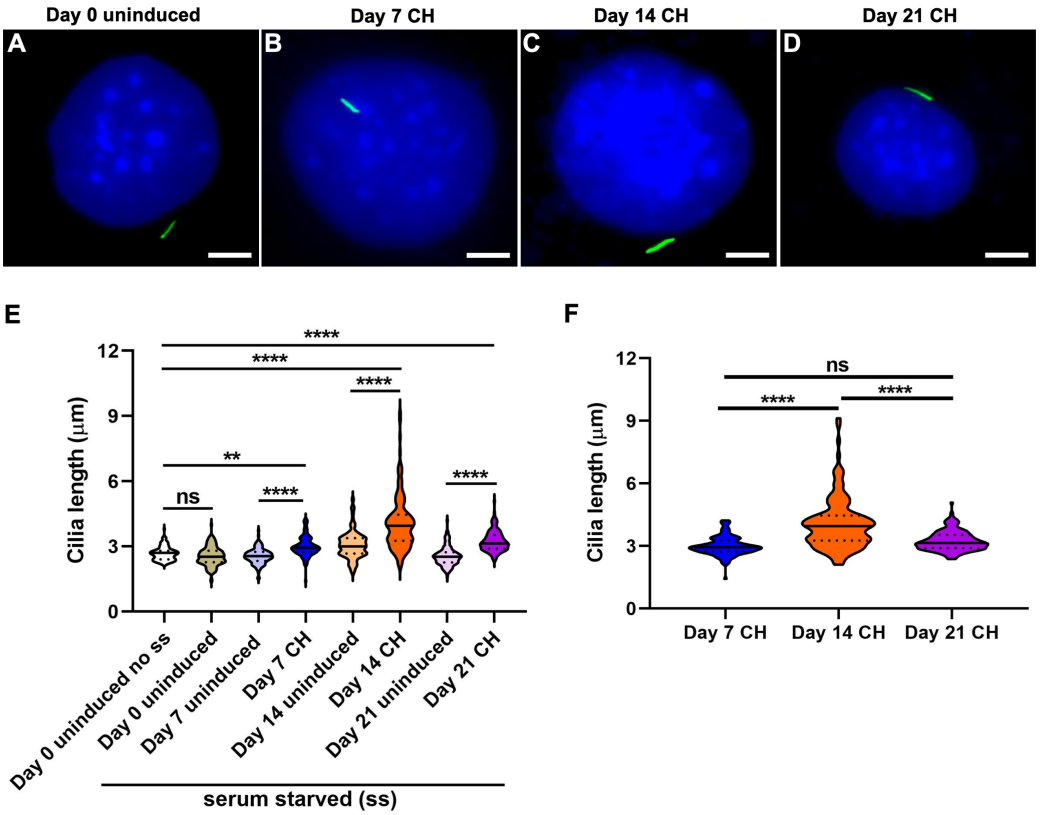

Figure 3 Chondrogenic differentiation causes elongation of primary cilia in ATDC5 cells. Two sets of undifferentiated cells were considered at day 0, namely non-serum starved (day 0 uninduced no ss) and starved (day 0 uninduced). All other CH differentiated and day matched uninduced cells were starved. (A–D) Representative images of ATDC5 primary cilium at day 0 uninduced and days 7, 14 and 21 after CH induction. Primary cilia were labeled with acetylated α tubulin (green), while nuclei were stained with DAPI (blue). Scale bar: five μm. (E) At days 7, 14 and 21 after CH differentiation primary cilia were significantly longer than day 0 and their day matched uninduced control cells. n = 110–152 ($^{**}p < 0.01$, $^{****}p < 0.0001$, One-way ANOVA followed by Tukey's post hoc test). (F) Among the CH induced cells, cilia were longest at day 14 ($^{****}p < 0.0001$, Two-way ANOVA followed by Tukey's post hoc test).
Full-size DOI: 10.7717/peerj.9799/fig-3

Cilia features demonstrate lineage and cell-type specific alteration in osteogenic and chondrogenic differentiation

We investigated the changes in primary cilia characteristics, for example, length and frequency over 21 days following CH and OS differentiation in ATDC5, C3H10T1/2 and MC3T3-E1 cells. Primary cilia length was discerned following immunolabeling with acetylated α tubulin. To ascertain the reliability of measurement we co-labeled cilia with its markers Arl13b and acetylated α tubulin in a subset of conditions and compared ciliary length detected with each marker in uninduced and induced monoloayers. We found no significant differences in cilia length reported by either marker in these cell-lines (Figs. S2–S4).

Chondrogenic induction results in primary cilia elongation in ATDC5 cells

Representative images for cells at day 0 uninduced and 7, 14 and 21 days CH differentiated cells are shown (Figs. 3A–3D; Fig. S5). Cilia length was increased at all time points following CH induction compared to day 0 and day matched uninduced controls but were longest after 14 days of differentiation (n = 110–152; One-way ANOVA followed by Tukey's post hoc test; Fig. 3E). Assessing specifically the induced group, showed that cilia in 14 day CH stimulated cells were significantly longer than in 7 and 21 day CH induced monolayers (Two-way ANOVA followed by Tukey's post hoc test; Fig. 3F). Significant variability in cilia length was noted between day 0 uninduced no ss and day 14 uninduced monolayers (One-way ANOVA followed by Tukey's post hoc test; Fig. S7A). We also found the CH induction effect to be significantly greater despite day specific variabilities in cilia length ($p < 0.0001$, Nested t test). Finally primary cilia frequency did not vary significantly during CH differentiation in ATDC5 cells (Fig. S8A).

Osteogenic differentiation was associated with cell-type specific changes in primary cilia length and incidence

C3H10T1/2 and MC3T3-E1 cells were treated to identical OS differentiation conditions. Cell-line specific changes in primary cilia length were noted and representative images are shown (Figs. 4, 5A–5D; Fig. S6). Both cell-lines showed variability in cilia length even in the absence of induction factors (Figs. S7B and S7C).

In C3H10T1/2, primary cilia in 14 day OS differentiated cells were significantly shorter compared to both day 0 and the corresponding day matched uninduced controls, but were longer than in 7 day OS induced cells (n = 111–177; One-way ANOVA followed by Tukey's post hoc test; Fig. 4E). Cilia appeared longest at 21 days post OS differentiation. Overall, cilia seemed to be progressively lengthened with sustained OS differentiation in this cell-line (Two-way ANOVA followed by Tukey's post hoc test; Fig. 4F). Preponderance of ciliated cells did not vary significantly during OS differentiation in C3H10T1/2 (Fig. S8B).

In MC3T3-E1, serum starvation caused significant increase in primary cilia length and incidence, including in uninduced cells at day 0 (Figs. 5E–5G). Nevertheless, cilia in 14 and 21 days OS media treated cells were significantly elongated, compared to day 0 and day matched uninduced cells (n = 101–178; One-way ANOVA followed by Tukey's post hoc test; Fig. 5E). Among OS media induced MC3T3-E1 cells, cilia were longer after 14 days of OS stimulation compared to 7 and 21 day differentiated cells (Two-way ANOVA followed by Tukey's post hoc test; Fig. 5F). At 21 days after OS induction, cilia prevalence in MC3T3-E1 was significantly reduced compared to day 0 and day matched uninduced cells, however no differences were observed at other time-points (n = 326–710; One-way ANOVA followed by Tukey's post hoc test; Fig. 5G). For both C3H10T1/2 and MC3T3-E1 despite day-wise cilia length variabilities (Figs. S7B and S7C) OS induction had a significant effect ($p < 0.001$ and $p < 0.0001$ respectively, Nested t test).

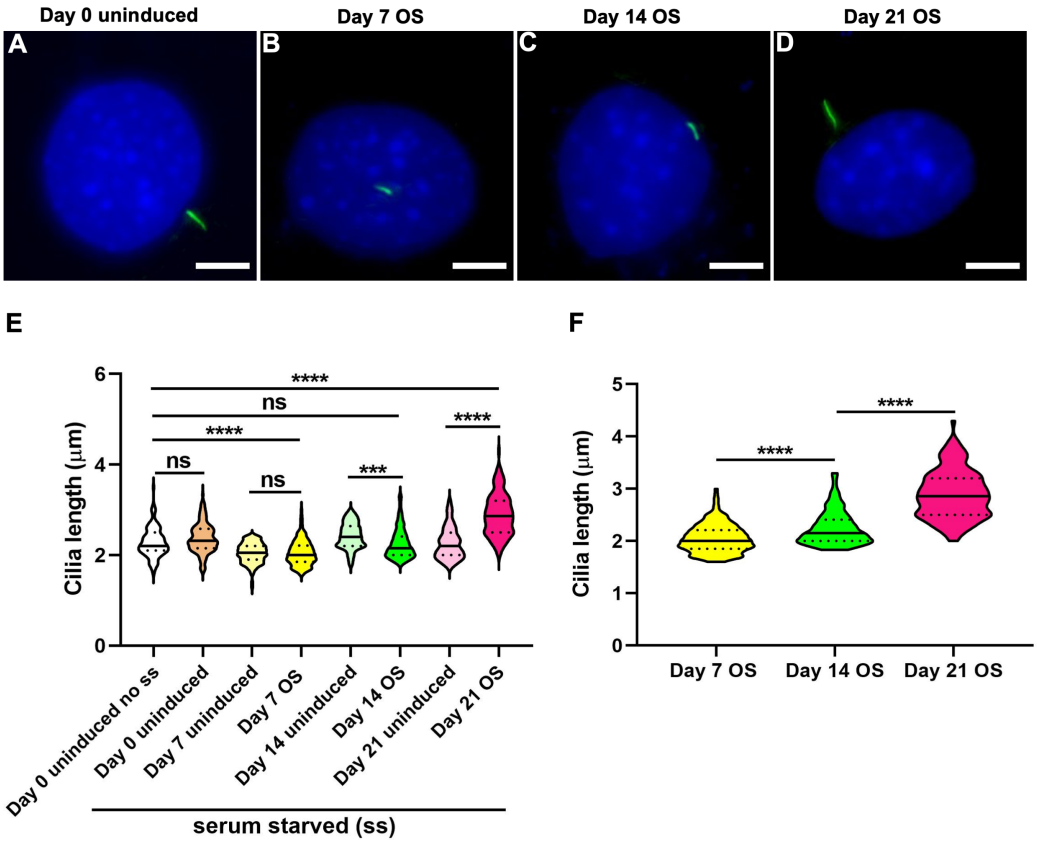

Figure 4 Osteogenic differentiation in C3H10T1/2 mesenchymal stem cells was associated with progressive cilia lengthening. (A–D) Representative images of primary cilium at day 0 uninduced and 7, 14 and 21 days OS induced cells. Primary cilia were labeled with acetylated α tubulin (green), while nuclei were stained with DAPI (blue). Scale bar: five μm. All differentiated and undifferentiated cells were serum starved (ss) except single set of uninduced cells at day 0 (day 0 uninduced no ss). (E) In day 7 OS differentiated cells primary cilia were significantly shorter than in day 0 uninduced; cilia were also shorter after 14 days of OS differentiation but were subsequently elongated in 21 day OS induced cells compared to day 0 and day matched uninduced cells. n = 111–177 (***$p < 0.001$, ****$p < 0.0001$, One-way ANOVA followed by Tukey's post hoc test). (F) Among the OS media treated cells, cilia were progressively elongated following differentiation that is, day 7 OS < day 14 OS < day 21 OS (****$p < 0.0001$, Two-way ANOVA followed by Tukey's post hoc test). Full-size DOI: 10.7717/peerj.9799/fig-4

SAG mediated Hedgehog activation is likely associated with increased cilia length and osteoblast differentiation in C3H10T1/2 cells

We assessed the mRNA expression levels of *Patched-1* (*Ptch1*), a direct target of Hh signaling, a canonical ciliary pathway in C3H10T1/2 cells. It was found to be significantly upregulated at 14 days and subsequently diminished at 21 days following OS induction (Fig. 6A). We then tested whether Hh stimulation via treatment with Smo agonist/SAG influenced ciliary characteristics during OS differentiation. SAG treatment alone for 7 days significantly upregulated *Alp* mRNA levels in C3H10T1/2 cells and this effect was further enhanced when combined with OS induction for the same period of time (Fig. 6B). In addition, SAG treatment with or without OS induction produced significant elongation of cilia compared to 7 day OS induced cells (n = 105–177; One-way ANOVA followed by

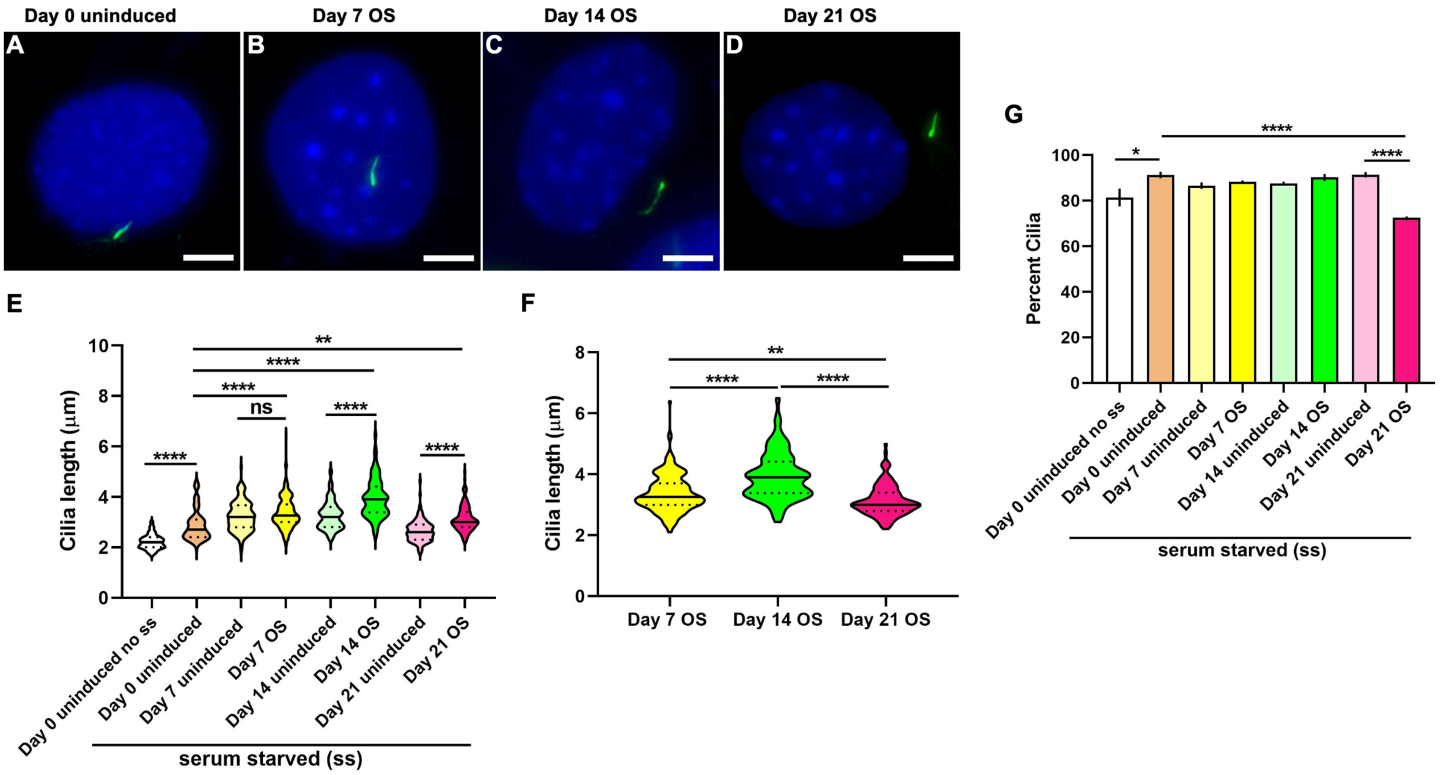

Figure 5 Osteogenic differentiation in MC3T3-E1 preosteoblast cells caused a distinct pattern of cilia elongation and reduction in frequencies. (A–D) Representative images of MC3T3-E1 primary cilium at day 0 uninduced and days 7, 14 and 21 after CH induction. Primary cilia were labeled with acetylated α tubulin (green), while nuclei were stained with DAPI (blue). Scale bar: five μm. All OS treated and untreated cells were serum starved (ss) except one set of uninduced cells at day 0 (day 0 uninduced no ss). (E) Serum starvation caused cilia length increase at day 0; at day 7 after osteogenesis cilia were longer than day 0 uninduced; at 14 and 21 days following OS differentiation the cilia are significantly longer than both day 0 and their corresponding day matched controls. n = 101–178 ($^{**}p < 0.01$, $^{****}p < 0.0001$, One-way ANOVA followed by Tukey's post hoc test). (F) Among OS media induced cells cilia were longest at 14 days of OS differentiation ($^{**}p < 0.01$, $^{****}p < 0.0001$, Two-way ANOVA followed by Tukey's post hoc test). (G) Starvation appeared to increase primary cilia prevalence in all induced and uninduced monolayers. However, cilia frequencies were significantly reduced only in 21 days OS differentiated cells, n = 326–710 ($^{*}p < 0.05$, $^{****}p < 0.0001$; One way ANOVA followed by Tukey's post hoc test).
Full-size DOI: 10.7717/peerj.9799/fig-5

Tukey's post hoc test; Fig. 6C). No change was observed in ciliary frequencies following SAG treatment (Fig. S8C).

DISCUSSION

Primary cilia are dynamically regulated sensory organelles that integrate diverse stimuli for mediating skeletal development and homeostasis. Ciliary properties, such as length and frequencies are often tightly correlated to cellular function. However, how cilia vary in native OS and CH differentiated monolayers in vitro is less understood. Here we characterized primary cilia features during 21 days of OS and CH differentiation in C3H10T1/2, MC3T3-E1 and ATDC5 cell-lines. In contrast to CH differentiation in hMSCs, which did not alter primary cilia length or shortened them in the presence of TGFβ3 (*Dalbay et al., 2015*), CH differentiation in ATDC5 cells without TGFβ3 caused cilia elongation (Fig. 3). The mean cilia length observed in non-starved day 0 uninduced ATDC5 cells (2.7 ± 0.03 μm) was similar to that in primary cultures of mouse fetal

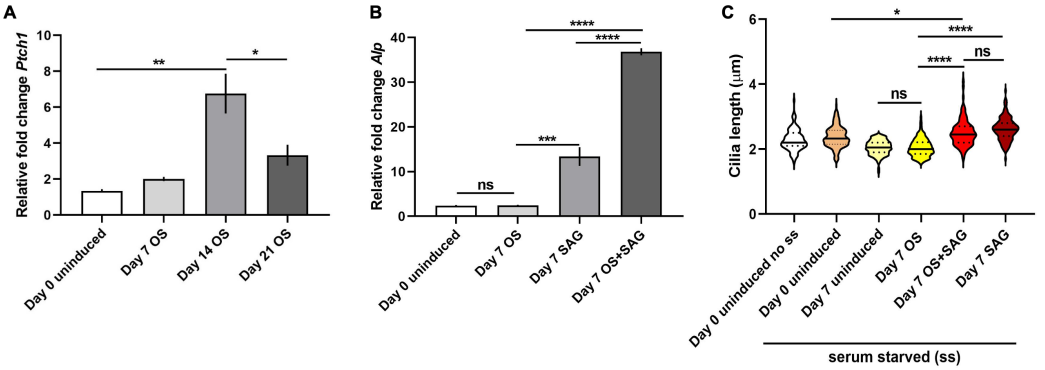

Figure 6 SAG treatment was associated with primary cilia elongation and increased osteoblast differentiation in C3H10T1/2 cells. (A and B) qRT-PCR analyses of the transcript levels of *Ptch1* and *Alp*. Levels were normalized to *Gapdh*. (A) mRNA levels of *Ptch1* was significantly elevated after 14 days of OS induction and then diminished at 21 days ($^{*}p < 0.05$, $^{**}p < 0.01$; One-way ANOVA followed by Tukey's post hoc analyses). (B) Both SAG treatment individually and combined with OS media for 7 days led to significant upregulation of *Alp* transcripts compared to day 7 OS differentiated cells; notably *Alp* levels were more strongly elevated with combinatorial SAG and OS induction as compared to SAG stimulation alone. ($^{***}p < 0.001$, $^{****}p < 0.0001$, One-way ANOVA followed by Tukey's post hoc test). (C) SAG treatment also resulted in significant elongation of primary cilia compared to day 0 uninduced and 7 day OS differentiated cells. $n = 105–177$ ($^{*}p < 0.05$, $^{****}p < 0.0001$, One-way ANOVA followed by Tukey's post hoc test). Full-size DOI: 10.7717/peerj.9799/fig-6

proliferative chondrocytes (2.82 ± 0.05 μm) but was longer than cilia in proliferative zone of mouse growth-plate cartilage (1.2 ± 0.01 μm) (*Martin et al., 2018*). CH differentiation was associated with lengthening of primary cilia at all time-points evaluated. Cilia were longest in 14 day CH differentiated cells (4.1 ± 0.11 μm) correlating with intermediate levels of differentiation, compared to those at day 7 (3 ± 0.04 μm) and day 21 (3.2 ± 0.04 μm) post CH induction (Figs. 2 and 3). Highest levels of matrix mineralization, GAG deposition and expression of *Mmp13*, a chondrocyte hypertrophy marker were noted at day 21 post CH induction. The proportion of ciliated non-starved day 0 control ATDC5 cells (83.9 ± 3%) were less compared to mouse fetal chondrocytes (92.6 ± 3.7%) (*Martin et al., 2018*). During CH differentiation in ATDC5 cells ciliary frequencies were not appreciably different and ranged from ~80% to 88% (Fig. S8A).

Dalbay et al. (2015) further reported that OS differentiation in hMSCs for seven days caused cilia length increase and reduction in frequencies. Primary cilia elongation has also been associated with elevated OS differentiation in other contexts (*Zhang et al., 2017*). Congruently, we observed cilia lengthening, although in a cell-type specific manner, during OS differentiation. The mean cilia length in non-starved day 0 uninduced MC3T3-E1 preosteoblasts (2.2 ± 0.03 μm) and C3H10T1/2 mesenchymal stem cells (2.3 ± 0.03 μm) were shorter compared to mouse primary osteoblasts (~2.9 μm) (*Lim et al., 2020b*). Cilia length in MLO-Y4 osteocytes have been reported to range from 2 μm to 4 μm (*Xiao et al., 2006*). In C3H10T1/2 cilia were longest in 21 day OS induced cells (2.9 ± 0.04 μm); at 14 day OS differentiation cilia (2.3 ± 0.03 μm) remained shorter than in controls but were elongated compared to in 7 days of osteogenesis (2.1 ± 0.02 μm) (Fig. 4). In MC3T3-E1, cilia lengths were significantly high in day 14 (3.9 ± 0.06 μm) and 21 (3.1 ± 0.05 μm)

OS differentiated cells vs controls but were longest in the former (Fig. 5). Frequencies of ciliated non-starved day 0 uninduced C3H10T1/2 (85.3 ± 2.6%) and MC3T3-E1 (81.4 ± 3.9%) cells were greater than in mouse primary osteoblasts (~70%) (*Lim et al., 2020b*). Notably the preponderance of ciliated cells significantly decreased in 21 day OS differentiated MC3T3-E1 cells compared to controls (72.5 ± 0.6%). In contrast, cilia incidence remained unchanged during osteogenesis in C3H10T1/2 and ranged from ~79% to 86% (Fig. S8B). It is noteworthy that significant OS differentiation was first evident after 14 days of OS induction and was highest after 21 days in both cell-lines (Fig. 1). These data reflect the occurrence of distinct cell-type specific molecular machineries that likely function by cilia modulation in disparate ways to elicit similar overall functional responses in each cell-line.

Our current approach of primary cilia length evaluation could be influenced by cells being seeded at a moderately lower density and on glass substrate for cilia immunodetection as compared to plastic for gene expression analyses, as well as cell morphology alterations coincident with differentiation. Furthermore cilia length in cultured cells could be influenced by several factors including differentiation media constituents. For example, dexamethasone that is widely utilized for promoting osteogenesis (*Derfoul et al., 2006*; *Langenbach & Handschel, 2013*; *Weiss et al., 2012*) is a potential enhancer of ciliogenesis and cilia length (*Forcioli-Conti et al., 2015*; *Khan et al., 2016*). However, its effect may be dosage dependent. In previous studies, cilia elongation has been observed with one µm and 10 µm dexamethasone with some effect being noted at concentrations as low as 10 nM (*Forcioli-Conti et al., 2015*; *Khan et al., 2016*). Despite this, using dexamethasone at identical concentrations to those employed here (100 nM), CH induction produced unaltered or shorter cilia, in hMSCs (*Dalbay et al., 2015*). This suggests that the inclusion of dexamethasone alone may not account for increased cilia length in all contexts. Testing each induction media component individually will be necessary to discern their role in cilia modulation, if any.

While specific mechanism(s) driving cilia length modulation in response to OS and CH differentiation here are unclear, length increase may be essential to enhance ciliary mechanosensitivity, signal transduction and promoting differentiated cell fates. Cilia elongation involves coordinated ciliary membrane extension and modulation of its composition. Longer cilia could experience greater membrane strain, stimulating opening of stretch-activated ion channels in the ciliary membrane or lead to increased bending energy at their base, triggering mechanotransduction signaling (*Resnick, 2015*; *Resnick & Hopfer, 2007*; *Schwartz et al., 1997*; *Spasic & Jacobs, 2017*). Increase in cilia length also enhances its surface area leading to accelerated synthesis and trafficking of cilia-specific proteins and signaling molecules to concentrate them in the ciliary microdomain for greater signaling activity (*Breslow et al., 2013*; *Kee et al., 2012*).

The Hh pathway performs essential roles in early limb bud patterning, stimulation of osteoblast differentiation in endochondral and intramembranous ossification and postnatal bone homeostasis (*Abzhanov et al., 2007*; *Horikiri et al., 2013*; *Kronenberg, 2003*; *Zhu et al., 2008*). The expression of Sonic hedgehog (Shh) was shown to be upregulated during OS differentiation in rat MSCs (*Ma et al., 2013*). In mammals, the cilium

forms an indispensable scaffold to concentrate Hh pathway components, modulating responsiveness to its ligands and regulating activator and repressor forms of the Glioma (Gli) family of transcription factors that control the expression of Hh-target genes (*Huangfu et al., 2003*; *Liu, Wang & Niswander, 2005*; *May et al., 2005*). Accordingly, Gli2 and Gli3 that are essential for mouse skeletal development (*Hui & Joyner, 1993*; *Mo et al., 1997*) and their proteolytic processing machinery localize at the cilium (*Haycraft et al., 2005*; *Mick et al., 2015*). Disruption of ciliary components, Ift80, Ift88 and Kif3a caused Gli2 depletion, in addition to defective OS differentiation, but osteogenesis was rescued by Gli2 overexpression (*Haycraft et al., 2007*; *Koyama et al., 2007*; *Yang & Wang, 2012*). In the present study we determined that the expression of *Ptch1*, a direct target and negative regulator of Hh signaling (*Carballo et al., 2018*), were increased in 14 day OS differentiated C3H10T1/2 cells but subsequently diminished after 21 days of OS stimulation (Fig. 6A). How increased *Ptch1* produces enhanced OS differentiation at 14 days is unclear but its subsequent decline in 21 day OS induced cells was indicative of potentially high Hh activity and was congruent with the highest levels of osteogenesis observed at this time-point. We treated C3H10T1/2 cells with SAG that can activate Smo, the essential transducer of Shh signaling by promoting its ciliary enrichment (*Chen et al., 2002*; *Frank-Kamenetsky et al., 2002*; *Rohatgi et al., 2009*). Alternatively, SAG may mediate Smo activation in a cilia independent manner (*Fan et al., 2014*). SAG stimulation individually and in combination with OS media treatment was associated with elevated *Alp* expression and significantly elongated cilia in 7 day OS differentiated cells (Figs. 6B and 6C). This is contrary to studies where SAG treatment in neuronal cell-types did not alter cilia length or neuronal activity (*Bansal et al., 2019*). Modifying cilia length in neural cell-types also did not alter Hh-dependent patterning (*Bangs et al., 2015*; *Bonnafe et al., 2004*). Notably Shh treatment has also been shown to potentiate OS differentiation in MC3T3-E1, C3H10T1/2, and ST2 cells (*Spinella-Jaegle et al., 2001*; *Tian et al., 2012*). These observations provide initial evidences likely suggesting that Hh activation could influence primary cilia properties and promote OS differentiation in C3H10T1/2, and mandate further dissection of its mechanistic basis.

In the current study we provide a detailed characterization of cilia features in OS and CH differentiated C3H10T1/2, MC3T3-E1 and ATDC5 cells. All cell-lines evaluated here have been extensively utilized to study molecular processes underlying osteoblast, chondrocyte differentiation and bone disorders, for example, osteoporosis and ciliopathies. It is noteworthy that skeletal ciliopathies such as short-rib thoracic dysplasias and cranioectodermal dysplasias are characterized by changes in primary cilia length and frequencies (*Dupont et al., 2019*; *Walczak-Sztulpa et al., 2010*). Moreover, degenerative conditions such as bone aging and osteoporosis are marked by the suppression of autophagy in osteocytes owing to their susceptibility to hypoxia and oxidative stress (*Onal et al., 2013*). Interestingly, primary cilia length modulation has been suggested to control autophagic activity in some contexts (*Pampliega et al., 2013*). Thus, modifying cilia length and thereby their sensory properties could serve as an attractive treatment modality in bone disorders. C3H10T1/2, MC3T3-E1 and ATDC5 have also been used in tissue engineering studies evaluating bone healing using various types of biomaterial scaffolds,

ultrasound frequencies, modulation of three dimensional cellular environment, static magnetic fields and growth factors (*Arosarena et al., 2011*; *Baudequin et al., 2017*; *Cicuendez et al., 2017*; *Martinez Sanchez et al., 2017*; *Matsumoto et al., 2018*; *Weiss et al., 2012*; *Yang et al., 2018*). In this premise, our data inform on the presence of stable cilia to orchestrate signaling during extended periods of OS and CH differentiation, in these cells. We report unique cell-line specific ciliary characteristics that could be useful to define lineage specific in vitro differentiation phenotypes. Our findings illustrate the dynamic variability in ciliary attributes in native differentiated cell-states. This can serve as a useful reference for studies using these cell-lines to dissect cilia dependent cellular processes or therapies for skeletal disorders involving cilia regulation. Finally our results shed light on the extent of basal variation in ciliary features in the absence of differentiation that may inform on the utility of these cell-lines and appropriate controls depending upon experimental goals. Overall these findings warrant in-depth delineation of the underlying regulatory mechanisms and signaling events in each cell-type.

CONCLUSION

We characterized the variation in primary cilia features, length and frequencies in ATDC5, C3H10T1/2 and MC3T3-E1 cells following CH and OS differentiation over 21 days. Briefly both were associated with elongation of cilia but displayed distinct alterations correlating with unique in vitro differentiated cell states. Reduced cilia frequencies were noted in 21 day OS differentiated MC3T3-E1 cells. Further investigations are needed to uncover the specific molecular processes governing the observed cell-line specific variations in cilia features during differentiation.

ACKNOWLEDGEMENTS

We are grateful to Dr. Uwe Kornak, Charité—Universitätsmedizin Berlin for providing us with ATDC5 and MC3T3-E1 cell-lines.

ADDITIONAL INFORMATION AND DECLARATIONS

Funding

This work was supported by an Early Career Research award (ECR/2016/001475) to Priyanka Upadhyai by the Science and Engineering Research Board, Department of Science and Technology, Government of India. Vishal Singh Guleria was supported by the Dr. TMA Pai PhD scholarship program by the Manipal Academy of Higher Education, Manipal, India. There was no additional external funding received for this study. The funders had no role in study design, data collection and analysis, decision to publish, or preparation of the manuscript.

Grant Disclosures

The following grant information was disclosed by the authors:
Science and Engineering Research Board: ECR/2016/001475.
Manipal Academy of Higher Education.

Competing Interests

The authors declare that they have no competing interests.

Author Contributions

- Priyanka Upadhyai conceived and designed the experiments, analyzed the data, prepared figures and/or tables, authored or reviewed drafts of the paper, and approved the final draft.
- Vishal Singh Guleria performed the experiments, analyzed the data, prepared figures and/or tables, and approved the final draft.
- Prajna Udupa performed the experiments, prepared figures and/or tables, and approved the final draft.

Data Availability

The following information was supplied regarding data availability:

Raw data for all figures are available as Supplemental Files and additional data are available as Supplemental Figures.

Supplemental Information

Supplemental information for this article can be found online at http://dx.doi.org/10.7717/peerj.9799#supplemental-information.

REFERENCES

Abzhanov A, Rodda SJ, McMahon AP, Tabin CJ. 2007. Regulation of skeletogenic differentiation in cranial dermal bone. *Development* **134**:3133–3144.

Arosarena OA, Del Carpio-Cano FE, Dela Cadena RA, Rico MC, Nwodim E, Safadi FF. 2011. Comparison of bone morphogenetic protein-2 and osteoactivin for mesenchymal cell differentiation: effects of bolus and continuous administration. *Journal of Cellular Physiology* **226**:2943–2952 DOI 10.1002/jcp.22639.

Bangs FK, Schrode N, Hadjantonakis AK, Anderson KV. 2015. Lineage specificity of primary cilia in the mouse embryo. *Nature Cell Biology* **17(2)**:113–122 DOI 10.1038/ncb3091.

Bansal R, Engle SE, Antonellis PJ, Whitehouse LS, Baucum AJ II, Cummins TR, Reiter JF, Berbari NF. 2019. Hedgehog pathway activation alters ciliary signaling in primary hypothalamic cultures. *Frontiers in Cellular Neuroscience* **13**:266 DOI 10.3389/fncel.2019.00266.

Baudequin T, Gaut L, Mueller M, Huepkes A, Glasmacher B, Duprez D, Bedoui F, Legallais C. 2017. The osteogenic and tenogenic differentiation potential of C3H10T1/2 (mesenchymal stem cell model) cultured on PCL/PLA electrospun scaffolds in the absence of specific differentiation medium. *Materials (Basel)* **10(12)**:1387 DOI 10.3390/ma10121387.

Berbari NF, Lewis JS, Bishop GA, Askwith CC, Mykytyn K. 2008. Bardet-Biedl syndrome proteins are required for the localization of G protein-coupled receptors to primary cilia. *Proceedings of the National Academy of Sciences* **105(11)**:4242–4246 DOI 10.1073/pnas.0711027105.

Besschetnova TY, Kolpakova-Hart E, Guan Y, Zhou J, Olsen BR, Shah JV. 2010. Identification of signaling pathways regulating primary cilium length and flow-mediated adaptation. *Current Biology* **20(2)**:182–187 DOI 10.1016/j.cub.2009.11.072.

Bhogaraju S, Cajanek L, Fort C, Blisnick T, Weber K, Taschner M, Mizuno N, Lamla S, Bastin P, Nigg EA, Lorentzen E. 2013. Molecular basis of tubulin transport within the cilium by IFT74 and IFT81. *Science* **341**:1009–1012 DOI 10.1126/science.1240985.

Bonnafe E, Touka M, AitLounis A, Baas D, Barras E, Ucla C, Moreau A, Flamant F, Dubruille R, Couble P, Collignon J, Durand B, Reith W. 2004. The transcription factor RFX3 directs nodal cilium development and left-right asymmetry specification. *Molecular and Cellular Biology* **24**:4417–4427 DOI 10.1128/mcb.24.10.4417-4427.2004.

Breslow DK, Koslover EF, Seydel F, Spakowitz AJ, Nachury MV. 2013. An in vitro assay for entry into cilia reveals unique properties of the soluble diffusion barrier. *Journal of Cell Biology* **203(1)**:129–147 DOI 10.1083/jcb.201212024.

Brown JA, Santra T, Owens P, Morrison AM, Barry F. 2014. Primary cilium-associated genes mediate bone marrow stromal cell response to hypoxia. *Stem Cell Research* **13(2)**:284–299 DOI 10.1016/j.scr.2014.06.006.

Cai JQ, Huang YZ, Chen XH, Xie HL, Zhu HM, Tang L, Yang ZM, Huang YC, Deng L. 2012. Sonic hedgehog enhances the proliferation and osteogenic differentiation of bone marrow-derived mesenchymal stem cells. *Cell Biology International* **36**:349–355 DOI 10.1042/CBI20110284.

Caplan AI, Correa D. 2011. PDGF in bone formation and regeneration: new insights into a novel mechanism involving MSCs. *Journal of Orthopaedic Research* **29(12)**:1795–1803 DOI 10.1002/jor.21462.

Carballo GB, Honorato JR, De Lopes GPF, De Sampaio e Spohr TCL. 2018. A highlight on Sonic hedgehog pathway. *Cell Communication and Signaling* **16**:11 DOI 10.1186/s12964-018-0220-7.

Chen G, Deng C, Li YP. 2012. TGF-beta and BMP signaling in osteoblast differentiation and bone formation. *International Journal of Biological Sciences* **8(2)**:272–288 DOI 10.7150/ijbs.2929.

Chen JC, Chua M, Bellon RB, Jacobs CR. 2015. Epigenetic changes during mechanically induced osteogenic lineage commitment. *Journal of Biomechanical Engineering* **137(2)**:020902 DOI 10.1115/1.4029551.

Chen JK, Taipale J, Young KE, Maiti T, Beachy PA. 2002. Small molecule modulation of smoothened activity. *Proceedings of the National Academy of Sciences* **99(22)**:14071–14076 DOI 10.1073/pnas.182542899.

Christensen ST, Clement CA, Satir P, Pedersen LB. 2012. Primary cilia and coordination of receptor tyrosine kinase (RTK) signalling. *Journal of Pathology* **226(2)**:172–184 DOI 10.1002/path.3004.

Cicuendez M, Silva VS, Hortiguela MJ, Matesanz MC, Vila M, Portoles MT. 2017. MC3T3-E1 pre-osteoblast response and differentiation after graphene oxide nanosheet uptake. *Colloids and Surfaces B: Biointerfaces* **158**:33–40 DOI 10.1016/j.colsurfb.2017.06.019.

Clement CA, Ajbro KD, Koefoed K, Vestergaard ML, Veland IR, Henriques de Jesus MP, Pedersen LB, Benmerah A, Andersen CY, Larsen LA, Christensen ST. 2013. TGF-beta signaling is associated with endocytosis at the pocket region of the primary cilium. *Cell Reports* **3**:1806–1814 DOI 10.1016/j.celrep.2013.05.020.

Cole DG, Diener DR, Himelblau AL, Beech PL, Fuster JC, Rosenbaum JL. 1998. Chlamydomonas kinesin-II-dependent intraflagellar transport (IFT): IFT particles contain proteins required for ciliary assembly in *Caenorhabditis elegans* sensory neurons. *Journal of Cell Biology* **141(4)**:993–1008 DOI 10.1083/jcb.141.4.993.

Dalbay MT, Thorpe SD, Connelly JT, Chapple JP, Knight MM. 2015. Adipogenic differentiation of hMSCs is mediated by recruitment of IGF-1r onto the primary cilium associated with cilia elongation. *Stem Cells* **33(6)**:1952–1961 DOI 10.1002/stem.1975.

Derfoul A, Perkins GL, Hall DJ, Tuan RS. 2006. Glucocorticoids promote chondrogenic differentiation of adult human mesenchymal stem cells by enhancing expression of cartilage extracellular matrix genes. *Stem Cells* **24**:1487–1495 DOI 10.1634/stemcells.2005-0415.

Dupont MA, Humbert C, Huber C, Siour Q, Guerrera IC, Jung V, Christensen A, Pouliet A, Garfa-Traore M, Nitschke P, Injeyan M, Millar K, Chitayat D, Shannon P, Girisha KM, Shukla A, Mechler C, Lorentzen E, Benmerah A, Cormier-Daire V, Jeanpierre C, Saunier S, Delous M. 2019. Human IFT52 mutations uncover a novel role for the protein in microtubule dynamics and centrosome cohesion. *Human Molecular Genetics* **28**:2720–2737 DOI 10.1093/hmg/ddz091.

Ezratty EJ, Stokes N, Chai S, Shah AS, Williams SE, Fuchs E. 2011. A role for the primary cilium in Notch signaling and epidermal differentiation during skin development. *Cell* **145(7)**:1129–1141 DOI 10.1016/j.cell.2011.05.030.

Failler M, Gee HY, Krug P, Joo K, Halbritter J, Belkacem L, Filhol E, Porath JD, Braun DA, Schueler M, Frigo A, Alibeu O, Masson C, Brochard K, Hurault de Ligny B, Novo R, Pietrement C, Kayserili H, Salomon R, Gubler MC, Otto EA, Antignac C, Kim J, Benmerah A, Hildebrandt F, Saunier S. 2014. Mutations of CEP83 cause infantile nephronophthisis and intellectual disability. *American Journal of Human Genetics* **94**:905–914 DOI 10.1016/j.ajhg.2014.05.002.

Fan CW, Chen B, Franco I, Lu J, Shi H, Wei S, Wang C, Wu X, Tang W, Roth MG, Williams NS, Hirsch E, Chen C, Lum L. 2014. The hedgehog pathway effector smoothened exhibits signaling competency in the absence of ciliary accumulation. *Chemistry & Biology* **21**:1680–1689 DOI 10.1016/j.chembiol.2014.10.013.

Federman M, Nichols G Jr. 1974. Bone cell cilia: vestigial or functional organelles? *Calcified Tissue Research* **17(1)**:81–85 DOI 10.1007/bf02547216.

Follit JA, Tuft RA, Fogarty KE, Pazour GJ. 2006. The intraflagellar transport protein IFT20 is associated with the Golgi complex and is required for cilia assembly. *Molecular Biology of the Cell* **17**:3781–3792 DOI 10.1091/mbc.e06-02-0133.

Forcioli-Conti N, Lacas-Gervais S, Dani C, Peraldi P. 2015. The primary cilium undergoes dynamic size modifications during adipocyte differentiation of human adipose stem cells. *Biochemical and Biophysical Research Communications* **458(1)**:117–122 DOI 10.1016/j.bbrc.2015.01.078.

Frank-Kamenetsky M, Zhang XM, Bottega S, Guicherit O, Wichterle H, Dudek H, Bumcrot D, Wang FY, Jones S, Shulok J, Rubin LL, Porter JA. 2002. Small-molecule modulators of hedgehog signaling: identification and characterization of smoothened agonists and antagonists. *Journal of Biology* **1**:10 DOI 10.1186/1475-4924-1-10.

Gregory CA, Gunn WG, Peister A, Prockop DJ. 2004. An Alizarin red-based assay of mineralization by adherent cells in culture: comparison with cetylpyridinium chloride extraction. *Analytical Biochemistry* **329(1)**:77–84 DOI 10.1016/j.ab.2004.02.002.

Haycraft CJ, Banizs B, Aydin-Son Y, Zhang Q, Michaud EJ, Yoder BK. 2005. Gli2 and Gli3 localize to cilia and require the intraflagellar transport protein polaris for processing and function. *PLOS Genetics* **1(4)**:e53 DOI 10.1371/journal.pgen.0010053.

Haycraft CJ, Zhang Q, Song B, Jackson WS, Detloff PJ, Serra R, Yoder BK. 2007. Intraflagellar transport is essential for endochondral bone formation. *Development* **134(2)**:307–316 DOI 10.1242/dev.02732.

Hino K, Zhao C, Horigome K, Nishio M, Okanishi Y, Nagata S, Komura S, Yamada Y, Toguchida J, Ohta A, Ikeya M. 2018. An mTOR signaling modulator suppressed heterotopic

ossification of fibrodysplasia ossificans progressiva. *Stem Cell Reports* **11**:1106–1119 DOI 10.1016/j.stemcr.2018.10.007.

Hoey DA, Kelly DJ, Jacobs CR. 2011. A role for the primary cilium in paracrine signaling between mechanically stimulated osteocytes and mesenchymal stem cells. *Biochemical and Biophysical Research Communications* **412(1)**:182–187 DOI 10.1016/j.bbrc.2011.07.072.

Horikiri Y, Shimo T, Kurio N, Okui T, Matsumoto K, Iwamoto M, Sasaki A. 2013. Sonic hedgehog regulates osteoblast function by focal adhesion kinase signaling in the process of fracture healing. *PLOS ONE* **8(10)**:e76785 DOI 10.1371/journal.pone.0076785.

Huangfu D, Liu A, Rakeman AS, Murcia NS, Niswander L, Anderson KV. 2003. Hedgehog signalling in the mouse requires intraflagellar transport proteins. *Nature* **426(6962)**:83–87 DOI 10.1038/nature02061.

Hui C-c, Joyner AL. 1993. A mouse model of Greig cephalo-polysyndactyly syndrome: the extra-toes J mutation contains an intragenic deletion of the Gli3 gene. *Nature Genetics* **3**:241–246.

Jiang S, Chen G, Feng L, Jiang Z, Yu M, Bao J, Tian W. 2016. Disruption of kif3a results in defective osteoblastic differentiation in dental mesenchymal stem/precursor cells via the Wnt signaling pathway. *Molecular Medicine Reports* **14**:1891–1900 DOI 10.3892/mmr.2016.5508.

Kee HL, Dishinger JF, Blasius TL, Liu CJ, Margolis B, Verhey KJ. 2012. A size-exclusion permeability barrier and nucleoporins characterize a ciliary pore complex that regulates transport into cilia. *Nature Cell Biology* **14(4)**:431–437 DOI 10.1038/ncb2450.

Khan NA, Willemarck N, Talebi A, Marchand A, Binda MM, Dehairs J, Rueda-Rincon N, Daniels VW, Bagadi M, Thimiri Govinda Raj DB, Vanderhoydonc F, Munck S, Chaltin P, Swinnen JV. 2016. Identification of drugs that restore primary cilium expression in cancer cells. *Oncotarget* **7**:9975–9992 DOI 10.18632/oncotarget.7198.

Kim J, Lee JE, Heynen-Genel S, Suyama E, Ono K, Lee K, Ideker T, Aza-Blanc P, Gleeson JG. 2010. Functional genomic screen for modulators of ciliogenesis and cilium length. *Nature* **464(7291)**:1048–1051 DOI 10.1038/nature08895.

Koyama E, Young B, Nagayama M, Shibukawa Y, Enomoto-Iwamoto M, Iwamoto M, Maeda Y, Lanske B, Song B, Serra R, Pacifici M. 2007. Conditional Kif3a ablation causes abnormal hedgehog signaling topography, growth plate dysfunction, and excessive bone and cartilage formation during mouse skeletogenesis. *Development* **134**:2159–2169 DOI 10.1242/dev.001586.

Kozhemyakina E, Lassar AB, Zelzer E. 2015. A pathway to bone: signaling molecules and transcription factors involved in chondrocyte development and maturation. *Development* **142(5)**:817–831 DOI 10.1242/dev.105536.

Kronenberg HM. 2003. Developmental regulation of the growth plate. *Nature* **423**:332–336.

Kunova Bosakova M, Varecha M, Hampl M, Duran I, Nita A, Buchtova M, Dosedelova H, Machat R, Xie Y, Ni Z, Martin JH, Chen L, Jansen G, Krakow D, Krejci P. 2018. Regulation of ciliary function by fibroblast growth factor signaling identifies FGFR3-related disorders achondroplasia and thanatophoric dysplasia as ciliopathies. *Human Molecular Genetics* **27**:1093–1105 DOI 10.1093/hmg/ddy031.

Lancaster MA, Schroth J, Gleeson JG. 2011. Subcellular spatial regulation of canonical Wnt signalling at the primary cilium. *Nature Cell Biology* **13(6)**:700–707 DOI 10.1038/ncb2259.

Langenbach F, Handschel J. 2013. Effects of dexamethasone, ascorbic acid and beta-glycerophosphate on the osteogenic differentiation of stem cells in vitro. *Stem Cell Research & Therapy* **4(5)**:117 DOI 10.1186/scrt328.

Lee SJ, Lee EH, Park SY, Kim JE. 2017. Induction of fibrillin-2 and periostin expression in Osterix-knockdown MC3T3-E1 cells. *Gene* **596**:123–129 DOI 10.1016/j.gene.2016.10.018.

Lim J, Li X, Yuan X, Yang S, Han L, Yang S. 2020a. Primary cilia control cell alignment and patterning in bone development via ceramide-PKCzeta-beta-catenin signaling. *Communications Biology* **3**:45 DOI 10.1038/s42003-020-0767-x.

Lim J, Li X, Yuan X, Yang S, Han L, Yang S. 2020b. Primary cilia control cell alignment and patterning in bone development via ceramide-PKCζ-β-catenin signaling. *Communications Biology* **3**:1–13.

Liu A, Wang B, Niswander LA. 2005. Mouse intraflagellar transport proteins regulate both the activator and repressor functions of Gli transcription factors. *Development* **132(13)**:3103–3111 DOI 10.1242/dev.01894.

Ma X, Zhang X, Jia Y, Zu S, Han S, Xiao D, Sun H, Wang Y. 2013. Dexamethasone induces osteogenesis via regulation of hedgehog signalling molecules in rat mesenchymal stem cells. *International Orthopaedics* **37**:1399–1404 DOI 10.1007/s00264-013-1902-9.

Malone AM, Anderson CT, Tummala P, Kwon RY, Johnston TR, Stearns T, Jacobs CR. 2007. Primary cilia mediate mechanosensing in bone cells by a calcium-independent mechanism. *Proceedings of the National Academy of Sciences* **104(33)**:13325–13330 DOI 10.1073/pnas.0700636104.

Martin L, Kaci N, Estibals V, Goudin N, Garfa-Traore M, Benoist-Lasselin C, Dambroise E, Legeai-Mallet L. 2018. Constitutively-active FGFR3 disrupts primary cilium length and IFT20 trafficking in various chondrocyte models of achondroplasia. *Human Molecular Genetics* **27**:1–13 DOI 10.1093/hmg/ddx374.

Martinez Sanchez AH, Feyerabend F, Laipple D, Willumeit-Romer R, Weinberg A, Luthringer BJC. 2017. Chondrogenic differentiation of ATDC5-cells under the influence of Mg and Mg alloy degradation. *Materials Science & Engineering C* **72**:378–388 DOI 10.1016/j.msec.2016.11.062.

Matsumoto K, Shimo T, Kurio N, Okui T, Ibaragi S, Kunisada Y, Obata K, Masui M, Pai P, Horikiri Y, Yamanaka N, Takigawa M, Sasaki A. 2018. Low-intensity pulsed ultrasound stimulation promotes osteoblast differentiation through hedgehog signaling. *Journal of Cellular Biochemistry* **119**:4352–4360 DOI 10.1002/jcb.26418.

May SR, Ashique AM, Karlen M, Wang B, Shen Y, Zarbalis K, Reiter J, Ericson J, Peterson AS. 2005. Loss of the retrograde motor for IFT disrupts localization of Smo to cilia and prevents the expression of both activator and repressor functions of Gli. *Developmental Biology* **287**:378–389 DOI 10.1016/j.ydbio.2005.08.050.

McGlashan SR, Jensen CG, Poole CA. 2006. Localization of extracellular matrix receptors on the chondrocyte primary cilium. *Journal of Histochemistry & Cytochemistry* **54(9)**:1005–1014 DOI 10.1369/jhc.5A6866.2006.

McGlashan SR, Knight MM, Chowdhury TT, Joshi P, Jensen CG, Kennedy S, Poole CA. 2010. Mechanical loading modulates chondrocyte primary cilia incidence and length. *Cell Biology International* **34(5)**:441–446 DOI 10.1042/CBI20090094.

McMurray RJ, Wann AK, Thompson CL, Connelly JT, Knight MM. 2013. Surface topography regulates wnt signaling through control of primary cilia structure in mesenchymal stem cells. *Scientific Reports* **3(1)**:3545 DOI 10.1038/srep03545.

Mick DU, Rodrigues RB, Leib RD, Adams CM, Chien AS, Gygi SP, Nachury MV. 2015. Proteomics of primary cilia by proximity labeling. *Developmental Cell* **35(4)**:497–512 DOI 10.1016/j.devcel.2015.10.015.

Mo R, Freer AM, Zinyk DL, Crackower MA, Michaud J, Heng H, Chik KW, Shi X-M, Tsui L-C, Cheng SH. 1997. Specific and redundant functions of Gli2 and Gli3 zinc finger genes in skeletal patterning and development. *Development* **124**:113–123.

Nauli SM, Alenghat FJ, Luo Y, Williams E, Vassilev P, Li X, Elia AE, Lu W, Brown EM, Quinn SJ, Ingber DE, Zhou J. 2003. Polycystins 1 and 2 mediate mechanosensation in the primary cilium of kidney cells. *Nature Genetics* **33**:129–137 DOI 10.1038/ng1076.

Newton PT, Staines KA, Spevak L, Boskey AL, Teixeira CC, Macrae VE, Canfield AE, Farquharson C. 2012. Chondrogenic ATDC5 cells: an optimised model for rapid and physiological matrix mineralisation. *International Journal of Molecular Medicine* **30(5)**:1187–1193 DOI 10.3892/ijmm.2012.1114.

Nonaka S, Tanaka Y, Okada Y, Takeda S, Harada A, Kanai Y, Kido M, Hirokawa N. 1998. Randomization of left-right asymmetry due to loss of nodal cilia generating leftward flow of extraembryonic fluid in mice lacking KIF3B motor protein. *Cell* **95**:829–837 DOI 10.1016/s0092-8674(00)81705-5.

O'Conor CJ, Leddy HA, Benefield HC, Liedtke WB, Guilak F. 2014. TRPV4-mediated mechanotransduction regulates the metabolic response of chondrocytes to dynamic loading. *Proceedings of the National Academy of Sciences* **111(4)**:1316–1321 DOI 10.1073/pnas.1319569111.

Omori Y, Zhao C, Saras A, Mukhopadhyay S, Kim W, Furukawa T, Sengupta P, Veraksa A, Malicki J. 2008. Elipsa is an early determinant of ciliogenesis that links the IFT particle to membrane-associated small GTPase Rab8. *Nature Cell Biology* **10**:437–444 DOI 10.1038/ncb1706.

Onal M, Piemontese M, Xiong J, Wang Y, Han L, Ye S, Komatsu M, Selig M, Weinstein RS, Zhao H, Jilka RL, Almeida M, Manolagas SC, O'Brien CA. 2013. Suppression of autophagy in osteocytes mimics skeletal aging. *Journal of Biological Chemistry* **288**:17432–17440 DOI 10.1074/jbc.M112.444190.

Orimo H. 2010. The mechanism of mineralization and the role of alkaline phosphatase in health and disease. *Journal of Nippon Medical School* **77(1)**:4–12 DOI 10.1272/jnms.77.4.

Ovchinnikov D. 2009. Alcian Blue/Alizarin red staining of cartilage and bone in mouse. *Cold Spring Harbor Protocols* **2009(3)**:pdb.prot5170 DOI 10.1101/pdb.prot5170.

Pampliega O, Orhon I, Patel B, Sridhar S, Diaz-Carretero A, Beau I, Codogno P, Satir BH, Satir P, Cuervo AM. 2013. Functional interaction between autophagy and ciliogenesis. *Nature* **502(7470)**:194–200 DOI 10.1038/nature12639.

Pazour GJ, Wilkerson CG, Witman GB. 1998. A dynein light chain is essential for the retrograde particle movement of intraflagellar transport (IFT). *Journal of Cell Biology* **141(4)**:979–992 DOI 10.1083/jcb.141.4.979.

Piperno G, Mead K. 1997. Transport of a novel complex in the cytoplasmic matrix of Chlamydomonas flagella. *Proceedings of the National Academy of Sciences* **94(9)**:4457–4462 DOI 10.1073/pnas.94.9.4457.

Pitaval A, Tseng Q, Bornens M, Thery M. 2010. Cell shape and contractility regulate ciliogenesis in cell cycle-arrested cells. *Journal of Cell Biology* **191(2)**:303–312 DOI 10.1083/jcb.201004003.

Porter ME, Bower R, Knott JA, Byrd P, Dentler W. 1999. Cytoplasmic dynein heavy chain 1b is required for flagellar assembly in Chlamydomonas. *Molecular Biology of the Cell* **10(3)**:693–712 DOI 10.1091/mbc.10.3.693.

Prosser SL, Morrison CG. 2015. Centrin2 regulates CP110 removal in primary cilium formation. *Journal of Cell Biology* **208(6)**:693–701 DOI 10.1083/jcb.201411070.

Qiu N, Xiao Z, Cao L, Buechel MM, David V, Roan E, Quarles LD. 2012. Disruption of Kif3a in osteoblasts results in defective bone formation and osteopenia. *Journal of Cell Science* **125(8)**:1945–1957 DOI 10.1242/jcs.095893.

Resnick A. 2015. Mechanical properties of a primary cilium as measured by resonant oscillation. *Biophysical Journal* **109(1)**:18–25 DOI 10.1016/j.bpj.2015.05.031.

Resnick A, Hopfer U. 2007. Force-response considerations in ciliary mechanosensation. *Biophysical Journal* **93(4)**:1380–1390 DOI 10.1529/biophysj.107.105007.

Rohatgi R, Milenkovic L, Corcoran RB, Scott MP. 2009. Hedgehog signal transduction by smoothened: pharmacologic evidence for a 2-step activation process. *Proceedings of the National Academy of Sciences* **106(9)**:3196–3201 DOI 10.1073/pnas.0813373106.

Scherft JP, Daems WT. 1967. Single cilia in chondrocytes. *Journal of Ultrastructure Research* **19**:546–555 DOI 10.1016/s0022-5320(67)80080-7.

Schwartz EA, Leonard ML, Bizios R, Bowser SS. 1997. Analysis and modeling of the primary cilium bending response to fluid shear. *American Journal of Physiology* **272(1)**:F132–F138 DOI 10.1152/ajprenal.1997.272.1.F132.

Signor D, Wedaman KP, Orozco JT, Dwyer ND, Bargmann CI, Rose LS, Scholey JM. 1999. Role of a class DHC1b dynein in retrograde transport of IFT motors and IFT raft particles along cilia, but not dendrites, in chemosensory neurons of living *Caenorhabditis elegans*. *Journal of Cell Biology* **147**:519–530 DOI 10.1083/jcb.147.3.519.

Singla V, Reiter JF. 2006. The primary cilium as the cell's antenna: signaling at a sensory organelle. *Science* **313(5787)**:629–633 DOI 10.1126/science.1124534.

Snow JJ, Ou G, Gunnarson AL, Walker MR, Zhou HM, Brust-Mascher I, Scholey JM. 2004. Two anterograde intraflagellar transport motors cooperate to build sensory cilia on *C. elegans* neurons. *Nature Cell Biology* **6(11)**:1109–1113 DOI 10.1038/ncb1186.

Song B, Haycraft CJ, Seo HS, Yoder BK, Serra R. 2007. Development of the post-natal growth plate requires intraflagellar transport proteins. *Developmental Biology* **305(1)**:202–216 DOI 10.1016/j.ydbio.2007.02.003.

Spasic M, Jacobs CR. 2017. Lengthening primary cilia enhances cellular mechanosensitivity. *European Cells and Materials* **33**:158–168 DOI 10.22203/eCM.v033a12.

Spinella-Jaegle S, Rawadi G, Kawai S, Gallea S, Faucheu C, Mollat P, Courtois B, Bergaud B, Ramez V, Blanchet AM, Adelmant G, Baron R, Roman-Roman S. 2001. Sonic hedgehog increases the commitment of pluripotent mesenchymal cells into the osteoblastic lineage and abolishes adipocytic differentiation. *Journal of Cell Science* **114**:2085–2094.

Temiyasathit S, Tang WJ, Leucht P, Anderson CT, Monica SD, Castillo AB, Helms JA, Stearns T, Jacobs CR. 2012. Mechanosensing by the primary cilium: deletion of Kif3A reduces bone formation due to loading. *PLOS ONE* **7**:e33368 DOI 10.1371/journal.pone.0033368.

Tian Y, Xu Y, Fu Q, Dong Y. 2012. Osterix is required for Sonic hedgehog-induced osteoblastic MC3T3-E1 cell differentiation. *Cell Biochemistry and Biophysics* **64**:169–176.

Tummala P, Arnsdorf EJ, Jacobs CR. 2010. The role of primary cilia in mesenchymal stem cell differentiation: a pivotal switch in guiding lineage commitment. *Cellular and Molecular Bioengineering* **3**:207–212 DOI 10.1007/s12195-010-0127-x.

Walczak-Sztulpa J, Eggenschwiler J, Osborn D, Brown DA, Emma F, Klingenberg C, Hennekam RC, Torre G, Garshasbi M, Tzschach A, Szczepanska M, Krawczynski M, Zachwieja J, Zwolinska D, Beales PL, Ropers H-H, Latos-Bielenska A, Kuss AW. 2010. Cranioectodermal dysplasia, Sensenbrenner syndrome, is a ciliopathy caused by mutations in the IFT122 gene. *American Journal of Human Genetics* **86**:949–956 DOI 10.1016/j.ajhg.2010.04.012.

Wang C, Yuan X, Yang S. 2013. IFT80 is essential for chondrocyte differentiation by regulating hedgehog and Wnt signaling pathways. *Experimental Cell Research* **319(5)**:623–632 DOI 10.1016/j.yexcr.2012.12.028.

Wang P, Dong R, Wang B, Lou Z, Ying J, Xia C, Hu S, Wang W, Sun Q, Zhang P, Ge Q, Xiao L, Chen D, Tong P, Li J, Jin H. 2019. Genome-wide microRNA screening reveals miR-582-5p as a mesenchymal stem cell-specific microRNA in subchondral bone of the human knee joint. *Journal of Cellular Physiology* **234**:21877–21888 DOI 10.1002/jcp.28751.

Wann AK, Knight MM. 2012. Primary cilia elongation in response to interleukin-1 mediates the inflammatory response. *Cellular and Molecular Life Sciences* **69**:2967–2977 DOI 10.1007/s00018-012-0980-y.

Weiss HE, Roberts SJ, Schrooten J, Luyten FP. 2012. A semi-autonomous model of endochondral ossification for developmental tissue engineering. *Tissue Engineering Part A* **18(13–14)**:1334–1343 DOI 10.1089/ten.TEA.2011.0602.

Wheway G, Schmidts M, Mans DA, Szymanska K, Nguyen TT, Racher H, Phelps IG, Toedt G, Kennedy J, Wunderlich KA, Sorusch N, Abdelhamed ZA, Natarajan S, Herridge W, Van Reeuwijk J, Horn N, Boldt K, Parry DA, Letteboer SJF, Roosing S, Adams M, Bell SM, Bond J, Higgins J, Morrison EE, Tomlinson DC, Slaats GG, Van Dam TJP, Huang L, Kessler K, Giessl A, Logan CV, Boyle EA, Shendure J, Anazi S, Aldahmesh M, Al Hazzaa S, Hegele RA, Ober C, Frosk P, Mhanni AA, Chodirker BN, Chudley AE, Lamont R, Bernier FP, Beaulieu CL, Gordon P, Pon RT, Donahue C, Barkovich AJ, Wolf L, Toomes C, Thiel CT, Boycott KM, McKibbin M, Inglehearn CF, Consortium, UK, University of Washington Center for Mendelian Genomics, Mendelian G, Stewart F, Omran H, Huynen MA, Sergouniotis PI, Alkuraya FS, Parboosingh JS, Innes AM, Willoughby CE, Giles RH, Webster AR, Ueffing M, Blacque O, Gleeson JG, Wolfrum U, Beales PL, Gibson T, Doherty D, Mitchison HM, Roepman R, Johnson CA. 2015. An siRNA-based functional genomics screen for the identification of regulators of ciliogenesis and ciliopathy genes. *Nature Cell Biology* **17**:1074–1087 DOI 10.1038/ncb3201.

Wren KN, Craft JM, Tritschler D, Schauer A, Patel DK, Smith EF, Porter ME, Kner P, Lechtreck KF. 2013. A differential cargo-loading model of ciliary length regulation by IFT. *Current Biology* **23(24)**:2463–2471 DOI 10.1016/j.cub.2013.10.044.

Xiao Z, Zhang S, Mahlios J, Zhou G, Magenheimer BS, Guo D, Dallas SL, Maser R, Calvet JP, Bonewald L, Quarles LD. 2006. Cilia-like structures and polycystin-1 in osteoblasts/osteocytes and associated abnormalities in skeletogenesis and Runx2 expression. *Journal of Biological Chemistry* **281**:30884–30895 DOI 10.1074/jbc.M604772200.

Yamakawa K, Iwasaki H, Masuda I, Ohjimi Y, Honda I, Saeki K, Zhang J, Shono E, Naito M, Kikuchi M. 2003. The utility of Alizarin red s staining in calcium pyrophosphate dihydrate crystal deposition disease. *Journal of Rheumatology* **30**:1032–1035.

Yang J, Zhang J, Ding C, Dong D, Shang P. 2018. Regulation of osteoblast differentiation and iron content in MC3T3-E1 cells by static magnetic field with different intensities. *Biological Trace Element Research* **184**:214–225 DOI 10.1007/s12011-017-1161-5.

Yang S, Wang C. 2012. The intraflagellar transport protein IFT80 is required for cilia formation and osteogenesis. *Bone* **51(3)**:407–417 DOI 10.1016/j.bone.2012.06.021.

Yao Y, Wang Y. 2013. ATDC5: an excellent in vitro model cell line for skeletal development. *Journal of Cellular Biochemistry* **114(6)**:1223–1229 DOI 10.1002/jcb.24467.

Yoshimura S, Egerer J, Fuchs E, Haas AK, Barr FA. 2007. Functional dissection of Rab GTPases involved in primary cilium formation. *Journal of Cell Biology* **178(3)**:363–369 DOI 10.1083/jcb.200703047.

Zhang J, Dalbay MT, Luo X, Vrij E, Barbieri D, Moroni L, De Bruijn JD, Van Blitterswijk CA, Chapple JP, Knight MM, Yuan H. 2017. Topography of calcium phosphate ceramics regulates

primary cilia length and TGF receptor recruitment associated with osteogenesis. *Acta Biomaterialia* **57**:487–497 DOI 10.1016/j.actbio.2017.04.004.

Zhang W, Taylor SP, Nevarez L, Lachman RS, Nickerson DA, Bamshad M, University of Washington Center for Mendelian Genomics Consortium, Krakow D, Cohn DH. 2016. IFT52 mutations destabilize anterograde complex assembly, disrupt ciliogenesis and result in short rib polydactyly syndrome. *Human Molecular Genetics* **25**:4012–4020 DOI 10.1093/hmg/ddw241.

Zhu J, Nakamura E, Nguyen M-T, Bao X, Akiyama H, Mackem S. 2008. Uncoupling Sonic hedgehog control of pattern and expansion of the developing limb bud. *Developmental Cell* **14**:624–632.